THE ASTROPHYSICAL JOURNAL, Vol. 158, October 1969

ABSORPTION-LINE FORMATION IN A SCATTERING PLANETARY ATMOSPHERE: A TEST OF VAN DE HULST'S SIMILARITY RELATIONS

JAMES E. HANSEN
Institute for Space Studies, Goddard Space Flight Center, NASA, New York
Received 1969 January 24

ABSTRACT

Van de Hulst's similarity relations, which reduce the problem of anisotropic scattering in a homogeneous atmosphere to one of isotropic scattering by scaling the optical thickness and the single-scattering albedo, are tested for line formation in clouds and hazes. The relations are shown to give good approximations for a useful range of scattering angles when k (the first characteristic exponent occurring in the solution of the transfer equation in unbounded media) is the basis for the scaling relations. Moreover, except for the center of strong lines, the results are nearly as accurate if the scaling factor were simply $(1 - \langle\cos\theta\rangle)$, where $\langle\cos\theta\rangle$ is the asymmetry factor of the phase function; this indicates that the mean free path of a photon in a planetary atmosphere is less by the factor $(1 - \langle\cos\theta\rangle)$ than the value determined from synthetic spectra under the assumption of isotropic scattering.

The above results indicate that the density of cloud particles on Venus is about 6 times greater than the value suggested by the synthetic-spectra calculations of Belton, Hunten, and Goody for isotropic scattering, if it is assumed only that the cloud particles are at least $\sim 1\ \mu$ in radius. This implies that the density of cloud particles on Venus is comparable with that of cirrus clouds on Earth, a conclusion in agreement with a recent conclusion of Potter.

The relation of the computations to Belton's theory for the curve of growth and for the phase effects in a cloudy planetary atmosphere is indicated; for scattering angles at which the similarity relations are valid, anisotropic scattering may be accounted for by simply scaling the single-scattering albedo obtained from the curve-of-growth analysis with isotropic scattering. However, the variation of equivalent width with phase angle is increased significantly by anisotropic scattering, and, within observational uncertainties, the use of realistic phase functions provides a probable explanation for a discrepancy between the theoretical and the observed phase effects.

I. INTRODUCTION

In order to interpret the spectrophotometric measurements of molecular absorption lines in the radiation scattered by planetary atmospheres, particularly the H_2O and CO_2 lines of Venus, it is necessary to solve a multiple-scattering problem as described by van de Hulst (1948), Chamberlain and Kuiper (1956), and Chamberlain (1965). Belton, Hunten, and Goody (1968) have computed synthetic spectra for a semi-infinite, homogeneous, isotropically scattering atmosphere and have made comparisons with detailed observations of Venus, thus obtaining atmospheric properties at the level of the scattering clouds. Although typical particles of clouds and hazes scatter with pronounced anisotropy, van de Hulst and Grossman (1968) have predicted that the results computed for anisotropic phase functions will be practically the same as for isotropic scattering provided that the single-scattering albedo and the optical thickness (in the case of a finite atmosphere) are scaled according to certain similarity relations. Potter (1969) has in fact observed that line profiles computed for a particular phase function for the cloud and for isotropic scattering may be brought into near coincidence if the computed curves are displaced as required; however, his method for determining the displacement requires solving the transfer equation with anisotropic scattering.

Our purpose is to compute the shape of a Lorentz absorption line in the radiation scattered by a homogeneous atmosphere for phase functions typical of clouds and hazes and to compare the results with those obtained for isotropic scattering by using van de Hulst's similarity relations; results are also given for isotropic scattering with the optical

thickness and single-scattering albedo unscaled for the sake of comparison. The computations are made for both strong and weak absorption lines, and the effects of integrating over the visible planetary disk, of absorption in the continuum, and of a finite optical thickness are considered.

II. COMPUTATIONAL PROCEDURE

a) Definitions

We will use essentially the notation and definitions of Belton *et al.* (1968) so that σ = scattering coefficient per unit volume, κ_c = absorption coefficient per unit volume in the continuum (which may be due to absorption in the scattering particles), and κ_ν = additional absorption coefficient per unit volume (due to the gas causing the absorption line). The single-scattering albedo in the continuum is then

$$\varpi_c = \frac{\sigma}{\kappa_c + \sigma}, \tag{1}$$

which is assumed to be constant over a line. The single-scattering albedo, including gaseous absorption, is given by

$$\varpi_\nu = \frac{\sigma}{\kappa_\nu + \kappa_c + \sigma}. \tag{2}$$

For the Lorentz line shape,

$$\kappa_\nu = \kappa_0\left[1 + \left(\frac{\nu - \nu_0}{\gamma}\right)^2\right]^{-1}, \tag{3}$$

where κ_0 is the gas absorption coefficient at the frequency ν_0 of the line center and γ is the Lorentz width of the line. The Lorentz line profile is often appropriate for the conditions in planetary atmospheres, and in any case the exact line shape is not essential for the purposes of this paper. If the single-scattering albedo at the line center in the absence of continuous absorption is represented by ϖ_0,

$$\varpi_0 = \frac{\sigma}{\kappa_0 + \sigma}, \tag{4}$$

then ϖ_ν may be expressed in terms of ϖ_0 by

$$\varpi_\nu = \left[\frac{1}{\varpi_0} + \frac{1 - \varpi_0}{\varpi_0(1 + X^2)}\right]^{-1}, \tag{5}$$

where $X \equiv (\nu - \nu_0)/\gamma$.

For comparison with spectroscopic observations, the quantity of interest is the ratio of intensities

$$\frac{I_\nu(\tau;\mu,\phi;\mu_0,\phi_0)}{I_c(\tau;\mu,\phi;\mu_0,\phi_0)} = \frac{S_\nu(\tau;\mu,\phi;\mu_0,\phi_0)}{S_c(\tau;\mu,\phi;\mu_0,\phi_0)}, \tag{6}$$

where, following Chandrasekhar (1960), τ is the optical thickness of the atmosphere, $(\mu_0 = |\cos\theta_0|,\phi_0)$ is the direction of incident solar radiation with reference to the local normal, (μ,ϕ) is the direction of the scattered radiation, and S is the scattering function of Chandrasekhar (1960, p. 20). The subscripts ν and c indicate that the intensities refer to the single-scattering albedos ϖ_ν and ϖ_c, respectively.

b) Phase Functions

In addition to isotropic scattering, computations are made with phase functions typical of clouds and hazes; the phase functions were kindly computed by H. Cheyney from Mie scattering theory for spherical water particles at ninety-six scattering angles

0(.2)5(2.5)180. The particle-size distributions employed were those recommended by Deirmendjian (1964) for cloud particles (distribution peak at diameter 8 μ) and haze particles (diameter $\sim$0.1 μ, Deirmendjian's model C). The computations were made for the wavelength 8189 Å, which is of special interest for H_2O absorption on Venus; however, the resulting phase functions (Fig. 1) are typical of those expected for cloud and haze particles throughout the visual and near-infrared regions.

c) Computing Method

The scattering functions may be conveniently obtained for an arbitrary phase function with the "double only" computing method described by Hansen (1969); in this variation of van de Hulst's (1963) doubling method the scattering function for a layer of thickness $\tau_0 \sim 2^{-25}$ is obtained directly from the phase function, since multiple scattering is negligible for a layer that thin, and the scattering functions for layers progressively a factor of 2 thicker are obtained from equations which are an expression of van de Hulst's doubling principle. The accuracy may be maintained as desired, and

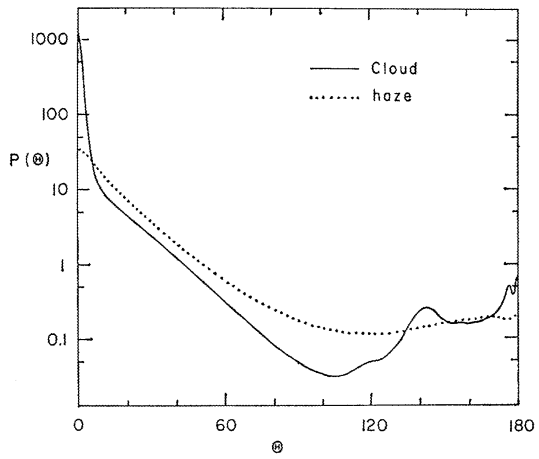

FIG. 1.—Single-scattering phase functions for cloud and haze particles

here we have attempted to keep the error less than about 0.3 percent, as indicated by several independent checks (Hansen 1969). The computations were carried to $\tau = 640$ (appropriate for limit $\tau \rightarrow \infty$) and the exact value of $\tau_0(10 \times 2^{-28})$ was chosen so that results for $\tau = 10$ were obtained as an intermediate result. Most of the line profiles were computed for either the incident or emergent direction normal to the surface, so that only the first (azimuth independent) term was required in the cosine expansion of the scattering function; however, for the results integrated over the planetary disk, intensities at all angles were needed, and in that case sixty terms were used for the phase function for the haze and 160 for the phase function for the cloud.

d) Similarity Relations

Van de Hulst and Grossman (1968) (see also van de Hulst 1968*a* for a more detailed presentation of his theory and van de Hulst 1968*b* for some numerical tests of its accuracy) have shown that the closest similarity between the radiation field reflected from an anisotropically scattering layer (of optical thickness τ and single-scattering albedo ϖ) and that reflected from an isotropically scattering layer (of optical thickness τ^i and single-scattering albedo ϖ^i) is obtained if the following similarity equations are obeyed:

$$k\tau = k^i\tau^i, \tag{7}$$

and

$$\frac{1-\varpi}{k} = \frac{1-\varpi^i}{k^i}, \tag{8}$$

where k is the exponent occurring in the solution of the transfer equation in unbounded media (i.e., $I(\tau \rightarrow \infty) \propto e^{-k\tau}$). The quantity k^i is related to ϖ^i through

$$\frac{1}{\varpi^i} = \frac{1}{2k^i} \log_e \left(\frac{1+k^i}{1-k^i}\right), \tag{9}$$

and k may be determined by solving an eigenvalue problem, although we obtain k with the doubling method from

$$k = \lim_{\tau \rightarrow \infty} \left\{\frac{1}{\tau} \log_e \left[\frac{t(\tau)}{t(2\tau)}\right]\right\}, \tag{10}$$

where $t(\tau)$ is the integral over all incident and emergent angles of Chandrasekhar's (1960, p. 20) transmission function. When the Henyey-Greenstein phase function is employed, the values obtained for $k(\varpi)$ agree with the table of van de Hulst and Grossman to the accuracy estimated by them, and the results for isotropic scattering are correct to several figures as indicated by equation (9).

e) Approximate Similarity Relations

According to van de Hulst (1968*a*), $(1 - \varpi)$ may be expanded in terms of k as

$$1 - \varpi = \frac{k^2}{3(1 - \langle \cos\theta \rangle)} + \ldots, \tag{11}$$

where the omitted terms are of order k^4 or higher and where $\langle \cos\theta \rangle$ is the anisotropy parameter of the phase function,

$$\langle \cos\theta \rangle = \tfrac{1}{2} \int_{-1}^{1} P(\cos\theta) \cos\theta d(\cos\theta), \tag{12}$$

which is 0 for isotropic scattering but 0.7430 and 0.8440, respectively, for the phase functions for the haze and for the cloud in Figure 1. For nearly conservative scattering, as in most weak lines, it should be a good approximation to neglect terms of order higher than k^2; in that case k and k^i may be eliminated from equations (7) and (8) to obtain the simple approximate similarity relations

$$\tau^i = \tau(1 - \langle \cos\theta \rangle), \tag{13}$$

and

$$1 - \varpi^i = \frac{1-\varpi}{1 - \langle \cos\theta \rangle}. \tag{14}$$

In line-formation problems it is the relative intensity that is of interest, and hence equations (13) and (14) may yield more accurate results than would otherwise be anticipated. The advantage of the approximate similarity relations (13) and (14) is that employment of them does not require knowledge of the function $k(\varpi)$. Figure 6 of van de Hulst and Grossman (1968) indicates that they have already tested and found accurate equation (13) for Henyey-Greenstein phase functions in the case of conservative scattering; for the same phase function in the case of nonconservative scattering a test of the accuracy of the similarity relations is contained in tables of the reflection function published by van de Hulst (1968*b*).

III. COMPUTATIONAL RESULTS

In all the graphs, where the separation of two curves would be less than about 1 percent of the vertical extent of the graph, the profiles are drawn as one curve. The four sets of line profiles in each of Figures 2, 3, 6, and 7 apply for the normal viewing direction ($\theta = 0°$) for incident directions $\theta_0 = 0°$, 30°, 60°, and 75°, or, what is the same thing, they apply for observation at the center of the planetary disk (sub-Earth point) for phase (Earth-planet-Sun) angles $\alpha = 0°$, 30°, 60°, and 75°; since the scattering function is symmetric in θ and θ_0 (Chandrasekhar 1960), the results are also valid for the incident and observation directions interchanged.

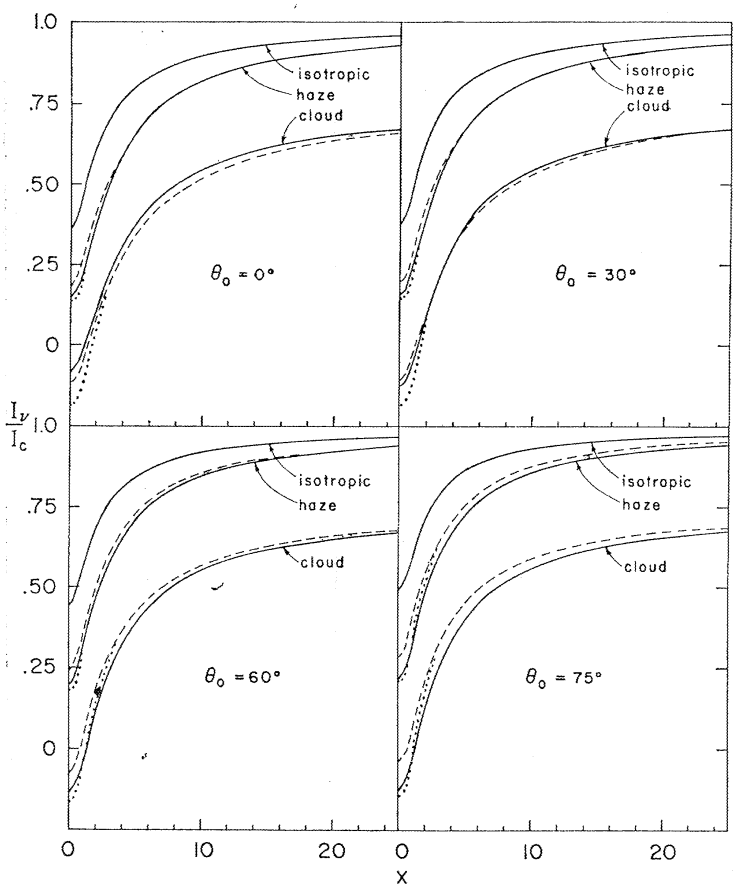

FIG. 2.—Absorption-line shape of a strong line ($\varpi_0 = 0.9$) for a thick atmosphere ($\tau = 640$) with no continuous absorption ($\varpi_c = 1.0$); for the normal emergent direction ($\theta = 0°$) and a range of incident directions (θ_0). *Solid line:* exact solution with no scaling applied; *dashed line:* solution from similarity equations (7) and (8); *dotted line:* solution from similarity equations (13) and (14). The results for the cloud are displaced downward by 0.25.

a) No Continuous Absorption

The line profiles for a thick atmosphere ($\tau = 640$) with no absorption in the continuum ($\varpi_c = 1$) are shown in Figure 2 for a strong line ($\varpi_0 = 0.9$) and in Figure 3 for a weak line ($\varpi_0 = 0.9975$). As compared with isotropic scattering, the line depths and equivalent widths are considerably increased for the phase function for the haze and still more for the phase function for the cloud as a consequence of their forward-throwing nature. However, the effects of secondary features in the phase functions are relatively

minor; the greatest effect occurs for the cloud at $\theta_0 = 0°$, where the 180° "halo" in the phase function causes an increase in the percentage of single-scattered photons and hence a decrease in the line strength.

For weak lines (Fig. 3), the exact (eqs. [7] and [8]) and approximate (eqs. [13] and [14]) similarity relations give indistinguishable results, both being a good approximation to the line profiles obtained with the anisotropic phase functions. Perhaps surprisingly, the results are almost as accurate for strong lines as for weak. The approximate relations

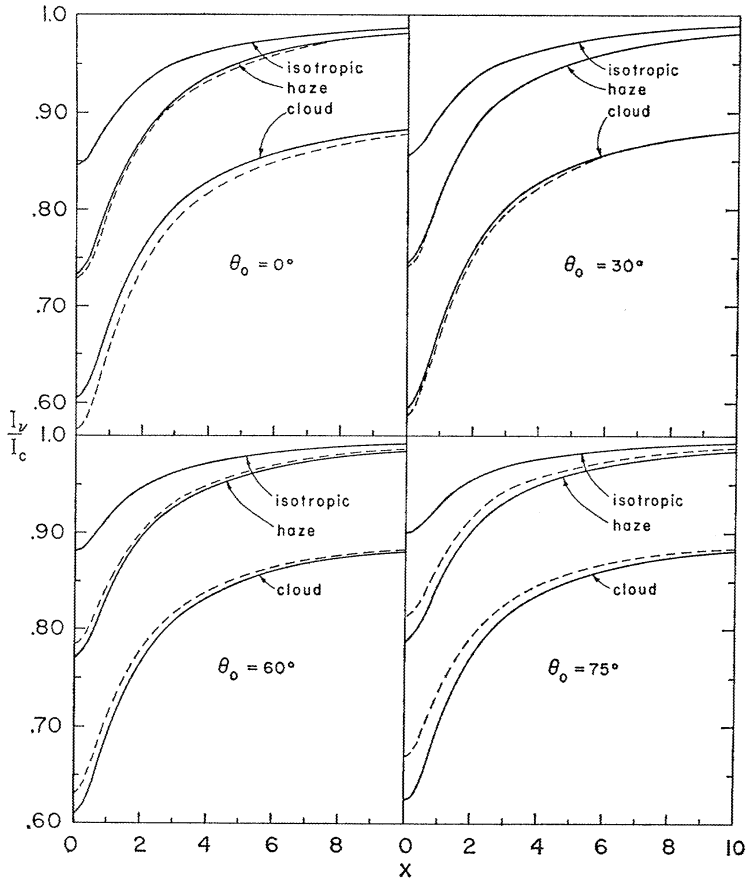

FIG. 3.—Same as Fig. 2 but for a weak line ($\varpi_0 = 0.9975$). The line profiles with the approximate (eqs. [13] and [14]) and exact (eqs. [7] and [8]) similarity relations are indistinguishable. The results for the cloud are displaced downward by 0.10.

do yield a line which is stronger near its center than it is for the true phase function for the cloud, but this is expected since $\varpi \to 0$ as $\langle \cos\theta \rangle \to \varpi$ (eq. [14]); in fact, with the approximate similarity relations, the line must be taken as being perfectly black for values of $\varpi < \langle \cos\theta \rangle$.

b) Integration over Planetary Disk

Observations often refer to the light integrated over the visible planetary disk; hence computations were also made for a thick atmosphere ($\tau = 640$) with no continuous absorption ($\varpi_c = 1$) for a strong line (Fig. 4) and for a weak line (Fig. 5). The conclusions are the same as in § III*a* except that for large phase angles ($a \gtrsim 125°$) neither set of similarity relations yields a useful approximation to the line profiles for phase functions for hazes and clouds. This is a result of the fact that toward large phase angles the

fraction of the observed photons which has been scattered only once (or a small number of times) becomes increasingly large, and the percentage of single-scattered photons that is absorbed does not depend on the shape of the phase function; it appears that at very large phase angles ($a \gtrsim 150°$) it is a better approximation to employ isotropic scattering with no scaling of ϖ or τ.

The problem which occurs at large phase angles also occurs, of course, for light not integrated over the planetary disk: if the scattering angle between the incident and emergent directions is $\lesssim 50°$, then the similarity relations result in lines which are much

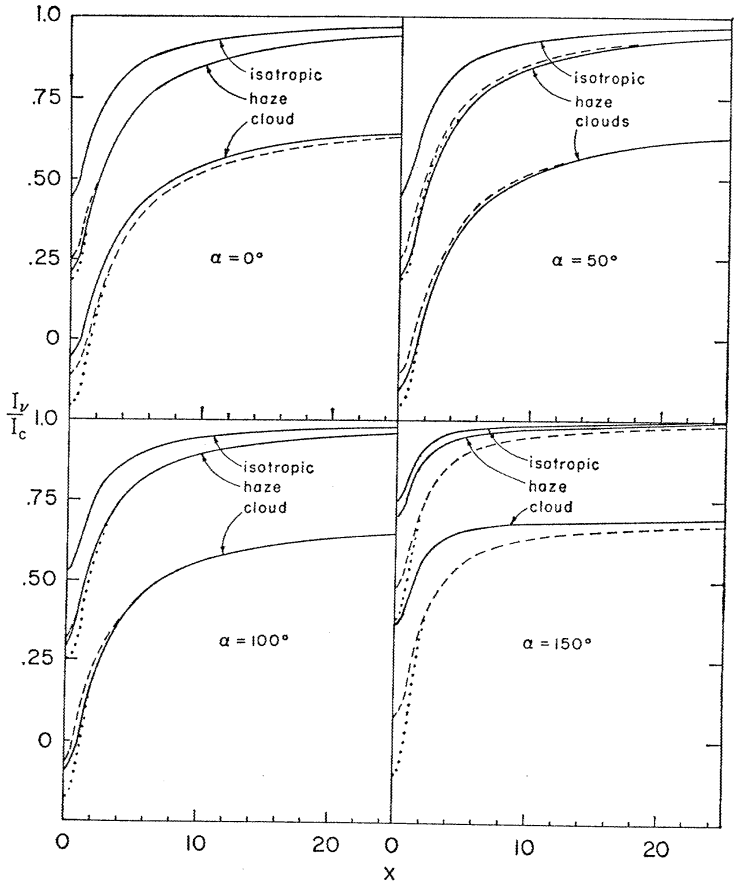

FIG. 4.—Same as Fig. 2 but for the light integrated over the visible planetary disk at the phase angle a. The results for the cloud are displaced downward by 0.30.

deeper than those calculated with the actual anisotropic phase functions. However, since localized measurements with near-grazing directions are difficult to perform, the limitation is less serious than it might appear.

c) Continuous Absorption

It is possible that the single-scattering albedo outside the line, ϖ_c, is less than unity; for example, the spherical albedo of Venus may be as low as ~ 0.7, and a small amount of continuous absorption could account for this. To test the effect of continuous absorption (which need not necessarily arise within the particles themselves), $\varpi_c = 0.976$, 0.9937, and 0.9962 have been used with the isotropic, haze, and cloud phase functions, respectively, since for $\tau = 640$ these single-scattering albedos lead to the common

spherical albedo 0.70. The required values for ϖ_c were obtained by trial and iteration, but note that, because of the large optical thickness, the values of the phase functions for hazes and clouds could have been obtained from the value for isotropic scattering by using equation (14).

The resulting line profiles for a strong line ($\varpi_0 = 0.9$) are shown in Figure 6. The lines are not as deep at the center, and the wings are much less pronounced than in the case of no continuous absorption (cf. Fig. 2), as has already been shown for isotropic

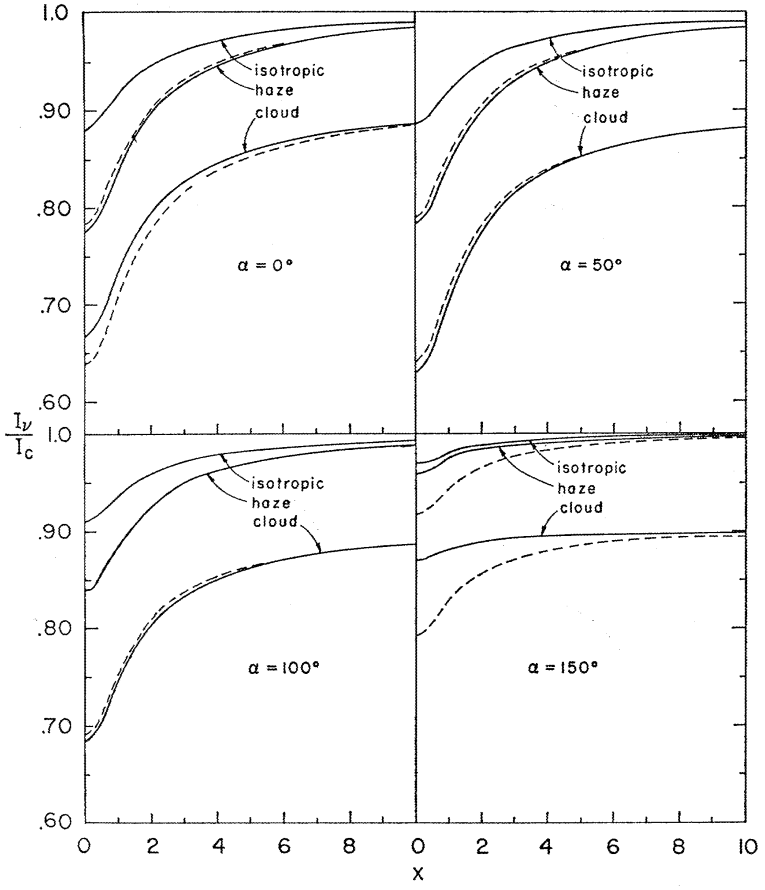

FIG. 5.—Same as Fig. 3 but for the light integrated over the visible planetary disk at the phase angle α

scattering by Belton *et al.* (1968). However, as expected, the addition of continuous absorption causes the line shapes computed with the similarity relations to be only slightly less accurate than in the case $\varpi_c = 1$.

d) Finite Atmosphere

In computing the results for an atmosphere of finite thickness it is important to include the variation of the total optical thickness across the line,

$$\tau_\nu = \tau_c \frac{\sigma + \kappa_\nu + \kappa_c}{\sigma + \kappa_c} = \tau_c \frac{\varpi_c}{\varpi_\nu} .$$

For an optical thickness in the continuum $\tau_c = 10$, the line profiles for a strong line with no continuous absorption are shown in Figure 7. As expected, the lines are not as deep as for $\tau = 640$ (Fig. 3), and the wings are much less pronounced. However, the similarity relations still provide useful approximations which are significantly better

than would be obtained by assuming isotropic scattering with no scaling of τ and ϖ. Although the accuracy of the similarity approximations decreases as τ decreases further, the spherical albedo in the continuum for $\tau_c = 10$ is already down to 0.55 and 0.67 with the phase functions for hazes and clouds, respectively, and these values are less than the spherical albedo of Venus.

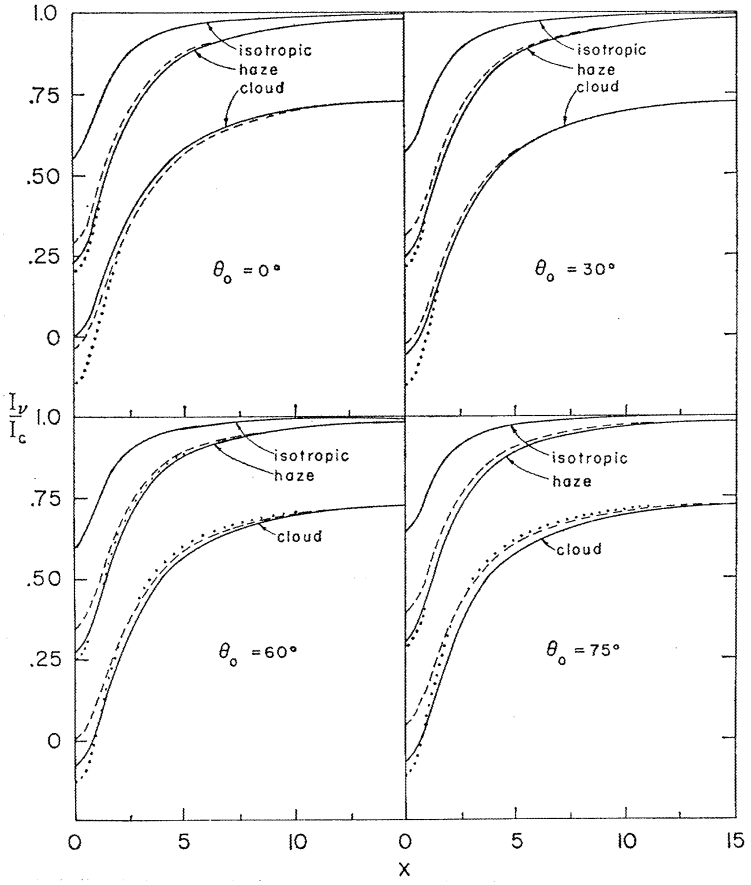

FIG. 6. Same as Fig. 2 but with continuous absorption ($\varpi_c = 0.976$, 0.9937, and 0.9962 for the isotropic, haze, and cloud phase functions, respectively) such that the planetary albedo in the continuum is 0.7. The results for the cloud are displaced downward by 0.25.

IV. CONCLUSIONS

The computations indicate that the strength of an absorption line formed in a scattering planetary atmosphere is considerably greater for phase functions typical of cloudy or hazy atmospheres than for isotropic scattering. However, by means of van de Hulst's similarity relations results can be obtained with isotropic scattering which provide a good approximation to the results with anisotropic scattering over a wide range of incident and emergent directions (for total scattering angles greater than about 50°). It should be emphasized that our computations have been made for the idealized case of a homogeneous planetary atmosphere, but this is an approximation that will probably continue to be made in many computations.

Potter (1969) has made the suggestion that conclusions based on the fitting of theoretical profiles computed for isotropic scattering to observational spectra may be modified to account for more realistic phase functions without actually recomputing all of the

synthetic spectra. Potter considers the case of a thick atmosphere and scales κ/σ rather than ϖ; although his approach should result in a nearly exact fit of the isotropic and anisotropic line profiles, it requires solving for at least one line profile for each anisotropic phase function for each set of incident and emergent angles. As shown below, van de Hulst's relations lead to conclusions in agreement with Potter's.

Although there is some uncertainty in the value of ϖ_c to be used for Venus, Belton *et al.* (1968) show that the possible values are limited to a small range, and by fitting

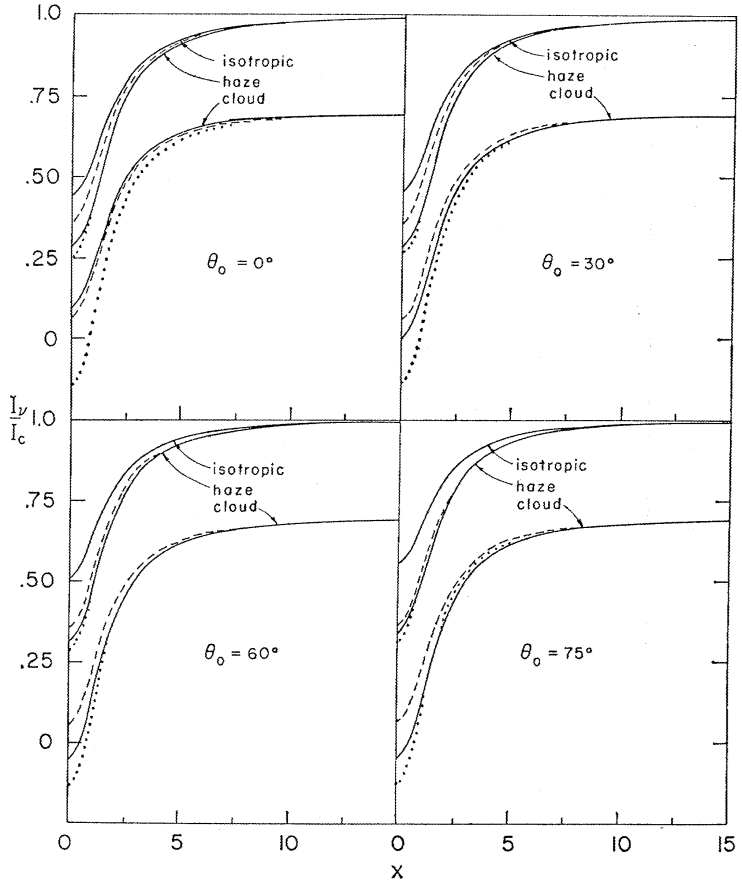

FIG. 7.—Same as Fig. 2 but for a finite atmosphere ($\tau_c = 10$). The results for the cloud are displaced downward by 0.30.

synthetic spectra (for isotropic scattering and a semi-infinite atmosphere) to their observations they derive ϖ_ν, which, through its dependence on κ_ν, is a function of the temperature and the pressure. If the cloud particles do not scatter isotropically, then similarity relation (14), which is valid except for strong lines, indicates that the derived value of $1 - \varpi_\nu$ should be multiplied by $1 - \langle\cos\theta\rangle$; however, for such lines (of weak or intermediate strength)

$$1 - \varpi_\nu = \frac{\kappa_\nu + \kappa_c}{\kappa_\nu + \kappa_c + \sigma} \simeq \frac{\kappa_\nu + \kappa_c}{\sigma} .$$

The synthetic spectra for anisotropic scattering will be nearly the same as for isotropic scattering, therefore, if κ_ν and κ_c (and the derived temperature and pressure) are unchanged and if σ is multiplied by $1/(1 - \langle\cos\theta\rangle)$; i.e., the results derived from isotropic scattering are unchanged except that the mean free path $\lambda = 1/(\sigma + \kappa_c) \sim 1/\sigma$

is multiplied by $1 - \langle\cos\theta\rangle$. Equivalently, M, the specific amount (the amount of gas traversed in one scattering mean free path; Belton [1968]), must be less by the factor $(1 - \langle\cos\theta\rangle)$ to produce the same synthetic spectra as for isotropic scattering. This is a result of the fact that, for a given density of cloud particles, the total path length of photons within the cloud is greater for a forward-scattering phase function than for isotropic scattering (Irvine 1968). Van de Hulst and Grossman (1968) and Potter (1969) have already suggested that the only significant change introduced by anisotropic scattering should be a change in the mean free path; a similar assumption was implicit in Chamberlain's (1965) approximation of ignoring the forward peak of the phase function.

The observations of Belton *et al.* (1968) were at incident and emergent angles well within the range of validity of the similarity relations. Therefore, if the cloud phase function is adopted for the Venus cloud particles, an assumption supported by computations of the visual phase curve by Arking and Potter (1968), then the mean free path of $\sim$1 km obtained by Belton *et al.* would be modified to 1 km $\times$ (1$-$0.854) $\simeq$ 0.15 km. The scale factor 0.146 is in excellent agreement with the values 0.134 and 0.169 derived by Potter (1969) from computations with the exact phase function for the cloud for two different absorption lines.

For spherical particles, $\langle\cos\theta\rangle$ is a function of the particle radius and the index of refraction, and its dependence on these parameters should be similar for randomly oriented nonspherical particles (J. M. Greenberg, private communication); water or ice particles with a dispersion of particle sizes and a mean radius greater than about 1 μ yield $\langle\cos\theta\rangle \sim 0.84 \pm 0.04$ at the wavelengths (0.8–1.1 μ) of interest (Irvine 1965; Hansen and Pollack 1969). If the index of refraction of the Venus cloud particles is 1.50 but the other conditions are unchanged, then $\langle\cos\theta\rangle \sim 0.80 \pm 0.05$; hence it appears that accounting for anticipated anisotropic scattering causes a significant change in the mean free path. According to references cited by Potter (1969), typical mean free paths in terrestrial cumulus and cirrus clouds are $\sim$0.01 and 0.13 km, respectively, values suggesting that in this respect the clouds of Venus may resemble cirrus clouds. However, this value for the mean free path is at best representative of conditions at the "level of line formation" in the real inhomogeneous atmosphere, and other observations, even in the same wavelength region, may refer to different levels; for example, observations of polarization and the extension of the cusps probably refer to higher, more diffuse regions.

Van de Hulst's similarity relations may be related to Belton's (1968) theory for the curve of growth and phase effects (variation of equivalent width with phase angle) in a cloudy atmosphere. Belton's formulae are valid for a homogeneous, semi-infinite, isotropically scattering atmosphere, and hence it is sufficient to recognize that the single-scattering albedos occurring in his theory correspond to ϖ^i above and should be scaled according to relation (8) or (14) if the phase function is not isotropic. This conclusion applies to observations at scattering angles for which the similarity relations are valid; therefore, as predicted by Belton, the inclusion of anisotropic scattering does not spoil the consistency he found between the observed and theoretical curves of growth for Venus. Also, since Earth-based observations of the major planets are necessarily made at small phase angles, the similarity relations are applicable to curve-of-growth theories for those planets.

However, the phase effect of Venus includes observations at large scattering angles at which the similarity relations do not hold, and hence to analyze the effects of anisotropic scattering requires computations with the actual phase functions. Belton's theory predicts that for isotropic scattering the ratio ($\equiv \Delta\phi$) of the equivalent width of a line at phase angle $\alpha = 50°$ to the equivalent width at $\alpha = 150°$ depends upon ϖ_c and upon whether the line is on the square-root, linear, or transition region on the curve of growth; from his Figure 6 we estimate the predictions for $\Delta\phi$ shown in Table 1.

As indicated by Belton, however, the observations by Moroz (1968) of CO_2 bands at 1.6 μ, for which the major lines are in the square-root region, yield $\Delta\phi \sim 3$, and the observations of Kuiper (1952) of CO_2 at 8689 Å, which may be in the transition region depending on the correct value of ϖ_c, yield $\Delta\phi \sim 12$. For isotropic scattering the observations are not consistent with any of the values of ϖ_c for which Belton made calculations ($\varpi_c \leq 0.999$).

A very crude estimate of the effect of anisotropic scattering may be made by noting from our calculations (§ III, Figs. 4 and 5) that (*a*) at $a = 150°$ the line equivalent widths are approximately the same for anisotropic scattering as for isotropic scattering, so that no transformation is required; and (*b*) at $a = 50°$ the similarity equations are valid, a fact which indicates that M, the specific amount, would be larger by the factor

TABLE 1

THEORETICAL RELATIVE PHASE VARIATION, $\Delta\phi$, FOR ISOTROPIC SCATTERING

	$\Delta\phi$	
ϖ_c	Linear	Square Root
0.999.....	3.8	1.9
0.98.....	2.2	1.5
0.90.....	1.7	1.3

TABLE 2

THEORETICAL RELATIVE PHASE VARIATIONS, $\Delta\phi$, FOR $1/(1-\langle\cos\theta\rangle) = 6$

	$\Delta\phi$	
ϖ_c	Linear	Square Root
0.999.....	22.8	4.8
0.98.....	13.2	3.6
0.90.....	10.5	2.2

$1/(1 - \langle\cos\theta\rangle) \sim 6$ for phase functions typical of clouds than for those typical of isotropic scattering.

From Belton's equations (8) and (12) it may be seen that anisotropic scattering increases the equivalent widths at $a = 50°$ by factors of approximately 6 and $\sqrt{6}$ in the linear and square-root regions, respectively, and hence phase functions typical of clouds lead to the predictions for $\Delta\phi$ shown in Table 2.

It appears that with anisotropic scattering the theoretical phase effect is in acceptable agreement with the observations for values of $\varpi_c \lesssim 0.999$. Belton (1968), in a note appended to his paper, indicates that if the scattering is almost exactly conservative ($1 - \varpi_c \ll 0.001$) and the atmosphere effectively semi-infinite, then the phase variation could be considerably increased even for isotropic scattering. However, since the phase function for Venus is certainly anisotropic, the above calculations at least indicate the importance of including the anisotropy in interpreting the phase effect. Because of the several uncertainties in this problem, the phase variation can not now yield a reliable value for ϖ_c.

Finally, we would like to emphasize that, at best, computations for a homogeneous atmosphere yield only certain average values for atmospheric properties, and, in addition, the validity of similarity relations for an inhomogeneous atmosphere has not been demonstrated. Since planetary atmospheres are necessarily inhomogeneous, owing primarily to variations with altitude of the pressure, temperature, and mixing ratio of particles to gas, it will therefore be necessary to compute synthetic spectra for a finite, inhomogeneous, anisotropically scattering atmosphere to derive *detailed* atmospheric properties from observed spectra. However, because of the time and effort required by such an undertaking, it appears that the similarity relations of van de Hulst may often provide a useful approximation to the results with anisotropic scattering.

I would like to thank Dr. Robert Jastrow, director of the Institute for Space Studies, for his hospitality. I am indebted to Dr. J. Potter for a preprint of his paper and to Drs. A. Arking, M. J. S. Belton, R. Goody, D. Hunten, W. Irvine, and H. C. van de Hulst for their comments on a draft version of this paper. During the course of this research the author held a National Research Council Postdoctoral Research Associateship supported by the National Aeronautics and Space Administration.

REFERENCES

Arking, A., and Potter, J. 1968, *J. Atm. Sci.*, **25**, 617.
Belton, M. J. S. 1968, *J. Atm. Sci.*, **25**, 596.
Belton, M. J. S., Hunten, D. M., and Goody, R. M. 1968, in *The Atmospheres of Venus and Mars*, ed. J. C. Brandt and M. B. McElroy (New York: Gordon & Breach), pp. 69–97.
Chamberlain, J. W. 1965, *Ap. J.*, **141**, 1184.
Chamberlain, J. W., and Kuiper, G. P. 1956, *Ap. J.*, **124**, 399.
Chandrasekhar, S. 1960, *Radiative Transfer* (New York: Dover Publishing Co.).
Deirmendjian, D. 1964, *Appl. Optics*, **3**, 187.
Hansen, J. E. 1969, *Ap. J.*, **155**, 565.
Hansen, J. E., and Pollack, J. B. 1969 (submitted to *J. Atm. Sci.*).
Hulst, H. C. van de. 1948, *Ap. J.*, **107**, 220.
———. 1963, NASA Institute for Space Studies Report (New York).
———. 1968*a*, *B.A.N.*, **20**, 77.
———. 1968*b*, *J. Comp. Phys.*, **3**, 777.
Hulst, H. C. van de, and Grossman, K. 1968, in *The Atmospheres of Venus and Mars*, ed. J. C. Brandt and M. B. McElroy (New York: Gordon & Breach), pp. 35–55.
Irvine, W. M. 1965, *J. Opt. Soc. Amer.*, **55**, 16.
———. 1968, *J. Quant. Spectrosc. and Rad. Transf.*, **8**, 471.
Kuiper, G. P. 1952, *The Atmospheres of the Earth and Planets*, ed. G. P. Kuiper (Chicago: University of Chicago Press), p. 306.
Moroz, V. I. 1968, *Soviet Astr.—AJ*, **11**, 653
Potter, J. F. 1969, *J. Atm. Sci.*, **26**, 511.